

have shown little conjugation between the sulfur atom and the phenyl ring but indicate potential S-N π bonding.(11) The properties of these systems have also been interpreted by invoking negative hyperconjugation as has been postulated in other X_3AY species such as O_3ClF and F_3SN .(7) Most notably, however, direct measurements to probe the degree of π bonding in such systems have not been reported.

We have previously shown that Sulfur K-edge X-ray Absorption Spectroscopy (S K-edge XAS) can be used as a direct probe of bonding in organosulfur species. The degree of π -bonding in S-nitrosothiols (RSNO) was shown in a clearly observable formal SN $\pi^* \leftarrow S_{1s}$ pre-edge transition supported by quantitatively determining the S_{3p} contributions.(12) (13) In particular, S K-edge XAS is selective for S_{3p} contributions to π -bonding in RSNO-type systems. The experimentally determined nature of the SN bond in S-nitrosothiols is also in good agreement with detailed computational studies on these species.(14) Herein, we investigate the electronic structure of sulfenato, sulfinato and sulfonato amide species using S K-edge XAS with complementary density functional theory (DFT) calculations. Our focus is specifically on defining the nature of the S-N bond and the impact of π_{SN} bonding.

Results

Sulfur K-edge XAS data were successfully obtained for three of the target compounds: **3a**, **2b**, and **3c** (see Figure 1A). Rapid X-ray photodegradation was observed for related compounds under the conditions of the experiments and cryoprotection was insufficient to prevent photoreduction; a limited number of experimental data are therefore available. The scope of the series was increased by computationally exploring the remainder of the compounds in Scheme 1. The intense characteristic ‘white line’ feature (dominated by $\sigma^*_{SX} \leftarrow S_{1s}$ contributions) occurs at 2477 eV for **2b** and about 4 eV higher in energy for the more oxidized **3a** and **3c**. This energy shift is similar to observed changes between sulfates and sulfonates(15) reflecting an increased Z_{eff} upon oxygenation. (16) The aryl sulfonate exhibits a low-energy shoulder (at 2479.4 eV) which is not present in the spectra of the alkyl species. This is consistent with similar features observed in aryl sulfonyl chlorides, which has previously been attributed to excited-state hyperconjugation with the aryl ring. (17) A weak feature visible at 2473 eV due to photoreduction is observed for **2b**. (18)

Time-dependent density functional theory (TD-DFT) calculations were performed on the complete series of compounds in Scheme 1, both for comparison with available experimental data and to

further explore the rest of the series. The simulated S K-edge XAS spectra yield overall good agreement with the experimental data (see Figure 1B).

For methanesulfonamide, **3a**, the lowest energy final states are dominated by σ^* contributions. Each of these final states fall into a narrow energy range leading to a single, intense feature corresponding to the white line in the S K-edge spectrum (see SI1). A more detailed analysis of the TD-DFT states reveal weak contributions from π^*_{SN} final states at similar energies to contributions from σ -type final states (see SI7-15), indicating mixed σ/π interactions from hyperconjugation. Such contributions are unresolvable in the experimental data and their contribution cannot be independently quantified experimentally. However, the lack of clearly discernible lower energy features in the spectrum, where π interactions would be expected, further indicate that direct S_{3p} contributions to π bonding are either not present or very weak.

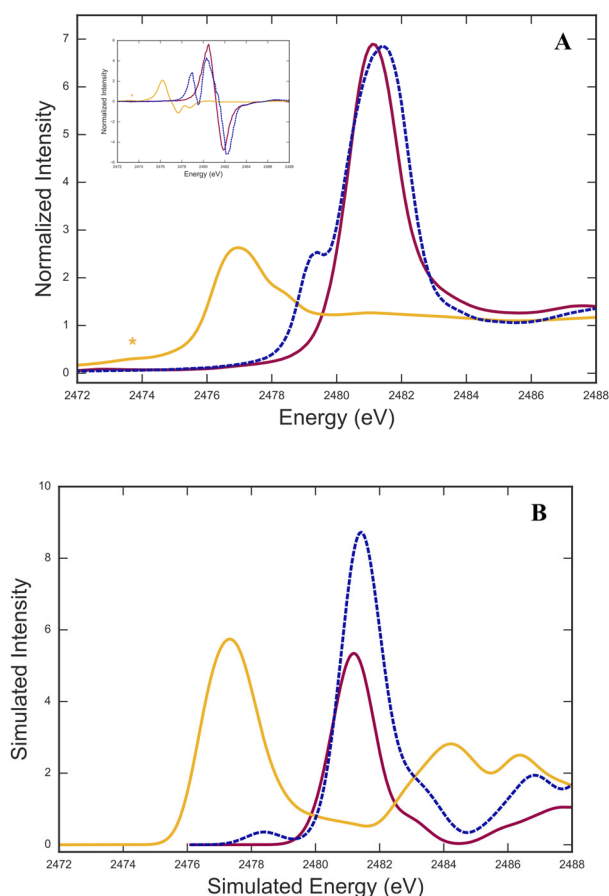


Figure 1: S K-edge XAS spectra (A) and their first-derivatives (A, inset) for compounds tertbutanesulfinamide (**2b**), methanesulfonamide (**3a**), and benzenesulfonamide (**3c**). A very weak feature (labeled with *) is observable in the pre-edge region for **2b** due to photoreduction in the beam. Spectra

have not been corrected for self-absorption effects. The TD-DFT simulated S K-edge XAS spectra (**B**) of tertbutanesulfinamide (**2b**), methanesulfonamide (**3a**), and benzenesulfonamide (**3c**). Overall simulated spectra are obtained by systematic broadening of all calculated transitions using a Gaussian lineshape with 1.3 eV FWHM, a reasonable approximation to that observed experimentally. Calculated final state energies for XAS simulations are also systematically shifted by +76 eV to offer better agreement with the experimental spectra (19).

Aryl substituents on the sulfonamide moiety (e.g., **3c**) have a significant impact on the S K-edge XAS spectra --- with the appearance of a relatively intense low-energy shoulder. Such a shoulder has also been observed in aryl sulfonyl chlorides (17) (as compared to their alkyl analogues) and reflects excited-state hyperconjugation with empty low-lying π^* states from the aryl ring. The poor agreement in the intensity of this shoulder likely reflects both self-absorption effects in the data and the limited ability of TD-DFT calculations to account for large electronic relaxation effects in the final states. Aside from this shoulder feature, contributions to the rest of spectra are very similar to **3a** (see SI2).

In the case of sulfinamides (e.g., **2b**), a large shift to lower energies and an overall drop in the intensity of the edge features is observed. Both of these effects correlate with a decrease in Z_{eff} , which together lower the energy of the core-level transitions and decreases the oscillator strength of $S_{3p} \leftarrow S_{1s}$ transitions. (19) The distribution of final states is very similar to those obtained for the alkylsulfonamide, with dominant contributions from σ^* final states and only minimal π^* contributions through hyperconjugation.

TD-DFT results for S_{1s} excitation in the complete series of compounds listed in Scheme 1 reveal additional trends depending on the oxidation state of the sulfur as well as the nature of the substituents (alkyl vs. aryl). Visual representations of these comparisons are given in SI4, SI5, SI6. Most notably, the white line feature that represents both σ^* contributions and hyperconjugative π^* contributions broaden from $RSO_2NH_2 \rightarrow RSONH_2 \rightarrow RSNH_2$. As a consequence of this effect, contributions to the S-N bond from hyperconjugation are predicted to decrease with deoxygenation due to poorer energy matching of the final states. The energy of the predicted excited-state hyperconjugation feature in the aryl species is well separated from the white line feature in the most oxidized species but is expected to merge with the white line in the more reduced sulfenamides, see SI6b.

Further computational studies on each of these S-N containing species were performed to estimate rotational barriers about the S-N bond ($\Delta E^{\text{rot}}_{\text{SN}}$), Table

1. There is surprisingly little difference between the rotational barriers as a function of the R substituent, in agreement with suggestions that sterics do not play a critical role in defining $\Delta E^{\text{rot}}_{\text{SN}}$. (9) (20) Oxidation at the sulfur centre has an overall greater impact on rotational barriers, particularly in the sulfonamides, which exhibit the lowest $\Delta E^{\text{rot}}_{\text{SN}}$.

Table 1: Calculated rotational energies about the S-N bond.

R	$\Delta E^{\text{rot}}_{\text{SN}}$ kJ/mol		
	RSNH ₂	RSONH ₂	RSO ₂ NH ₂
CH ₃	25.2	26.4	14.8
C(CH ₃) ₃	29.1	22.9	16.6
C ₆ H ₅	30.1	26.4	14.3
average	28.1 ± 2.6	25.2 ± 2.0	15.2 ± 1.2

Discussion

S K-edge XAS provides an opportunity to evaluate potential π contributions to bonding in S-N containing species. Given the atomic selection rules that generally govern core spectroscopy, S K-edge XAS is particularly selective to S_{3p} final state contributions and thus provides a direct experimental probe of contributions to bonding from valence p states. The data we have collected are readily supported by TDDFT calculations, allowing us to explore the broader implications of our results. Our experimental XAS data as well as TD-DFT calculations confirm that sulfonamides, sulfinamides, and sulfenamides have essentially no S-N π bonding involving S_{3p} contributions. Mulliken population analysis and electron density distributions in the x-ray final states (corresponding to the lowest-unoccupied states) also indicate no π contributions to bonding (see SI4b, SI5b, SI6b). The only notable exception is the presence of significant sulfur-carbon π_{SC} contributions in the lowest-energy final states for species with aryl substitution (**1c**, **2c**, and **3c**). This π delocalization into the phenyl ring is analogous to that which has been observed in other aryl sulfonyl species and is an excited state phenomenon. $RS(O)_nNH_2$ moieties show no spectroscopic evidence of S_{3p} contributions to π bonding in any of the investigated species.

As has been previously noted, (8) (20) the rotational barriers along the S-N axis differ markedly as a function of the oxidation state of the sulfur atom. We have, therefore, further explored the nature of the rotational barrier in these species, in greater detail, using DFT calculations. The calculated energies indicate an increase in barriers to rotation upon deoxygenation of the sulfur atom for all R-groups, Table 1, although these are small in all cases. The

geometry at the minimum energy for all sulfenamide species occurs around the 60° H-N-S-C dihedral angle, where the nitrogen lone pair is anti to the sulfur-R-group bond, Figure 2. At maximum energy the nitrogen lone pair is eclipsed with one of the sulfur lone pairs. Similarly, for the sulfonamide species, the minimum occurs when the nitrogen lone pair is anti to the R-group and the sulfur-oxygen bonds are gauche to the amide hydrogens. Both the sulfinamide and sulfonamide maximum energy configurations are similar to the eclipsed structure of the sulfenamides. A slight difference in configuration is seen at the sulfinamide minimum, where the R-group is gauche and the S-O bond is anti to the nitrogen lone pair, respectively.

Comparisons of the SN electronic and geometric descriptions at both maximum and minimum energy geometries show relatively small differences. The largest effect is observed in the S-N bond distances, which elongate by ~ 6 pm in the sulfenamides during bond rotation. This elongation is smaller for the sulfinamides (~ 4 pm) and even shorter for the sulfonamides (~ 2 pm). These structural differences do not reflect any substantial differences in SN bonding in different conformers. We find only very small electron density changes during rotation, suggesting that the nature of the bond is not affected, SI Table 1, and thus implying little to no π contributions in this bond. Taken together, our results support previous proposals that rotational barriers are dominated by electron repulsion. We note that experimental validation of the lack of d-p π interactions cannot be offered based on S K-edge studies and we are currently exploring the use of S L-edge spectroscopy to address this specific point with greater clarity.

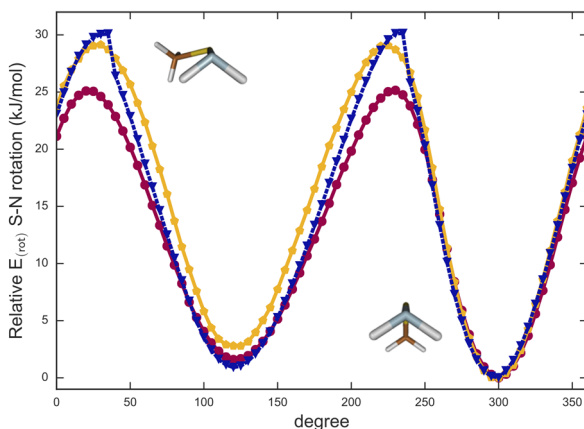


Figure 2: 360° rotation of R-groups; tertbutane (\blacklozenge), methane (\bullet), and benzene (\blacktriangledown) about the sulfur-nitrogen bond, for the sulfenamide species. Representative geometry for methanesulfenamide at respective maximum and minimum. For all other species please see SI Figure 7.

Table 2: Calculated S-N bond length during rotation about S-N bond, at local minimum and maximum, in Å.

	1a	1b	1c	2a	2b	2c	3a	3b	3c
S-N min	1.74	1.74	1.70	1.74	1.73	1.71	1.73	1.73	1.69
S-N max	1.81	1.78	1.72	1.81	1.78	1.73	1.79	1.79	1.72

Conclusions

Sulfenamides and its reduced congeners have historically been particularly difficult moieties to study due to a lack of methods for direct measurement. By applying S K-edge XAS to directly investigate how the sulfur atom interacts with its nearest neighbors we can gain an insight into the nature of the sulfur-nitrogen bond of sulfinated amides. Our studies point to minimal π -contributions in the sulfur-nitrogen bond.

Experimental

Materials

Methanesulfonamide (98% purity) and benzenesulfonamide ($\geq 98\%$ purity) were purchased from Sigma-Aldrich. Methanesulfonamide: ^1H NMR (300 MHz, DMSO) δ 2.91 (s, 3H, CH_3), δ 6.80 (s, 2H, NH_2); Benzenesulfonamide: ^1H NMR (300 MHz, DMSO) δ 7.83 (d, 2H, $J=6\text{Hz}$), δ 7.58 (m, 3H), δ 7.35 (s, 2H). Tertbutanesulfinamide (Ellman's sulfinamide) were synthesized in the laboratory of Scott Bohle at McGill University.

XAS Acquisition and Data Analysis

Sulfur K-edge XAS data for tertbutanesulfinamide were acquired at Stanford Synchrotron Radiation Lightsource (SSRL). Fluorescence data were collected at beamline 4-3 at the Stanford Synchrotron Radiation Lightsource (SSRL) under ring conditions of 3 GeV and 200-500 mA. Solid samples were mixed 1:1 with boron nitride, finely ground, to minimize self-absorption, and mounted as a thin layer on sulfur-free Kapton tape at room temperature. Fluorescence data were acquired using solid state detector at ambient temperature and pressure. Energy calibration was carried out using sodium thiosulfate ($\text{Na}_2\text{S}_2\text{C}_3$) with the first pre-edge feature being calibrated at 2472.02 eV (21).

Sulfur K-edge XAS data for methanesulfonamide and benzenesulfonamide were acquired at the Canadian Light Source. Total electron yield data were acquired at beamline SXRMB at the CLS under ring conditions of 3 GeV and 180-250 mA. Solid samples were mixed 1:1 with boron nitride, finely ground and mounted onto a copper sample holder with carbon tape. Total electron yield data were acquired under

vacuum at ambient temperature. Calibrations were performed as above.

Raw data were normalized to incoming beam (I_0), calibrated and averaged with the Blueprint-XAS (22) prefit function. Only the first scans of tert-butanesulfonamide were used due to sulfur photoreduction in the fluorescence data. As TEY does not exhibit such photoreduction, all scans per run of the two sulfonamides were averaged for greater signal-to-noise ratio. Background subtraction and normalization of the spectra were achieved using BlueprintXAS (23). The number of components for fits were estimated by employing the Akaike information criterion (AIC) (24) (25). The model with the lowest AIC was chosen for fitting of all spectra; fits with smallest sum of squared errors were chosen for background subtraction and normalization which lead to the data shown in this paper.

Self-absorption corrections were not applied to the XAS data obtained for **2b**, **3a**, and **3c**; for this reason, detailed intensity analyses of the data were not performed.

DFT

All gas phase DFT calculations were run using ORCA, version 2.9.0 (26), using spin-unrestricted Kohn-Sham equations with BP86 functional and TZVP basis set. No relativistic effects were added. Excited state calculations and XAS simulations were conducted with TDDFT and XES. The energies calculated for XAS simulations are shifted by +76 eV to match with the experimental spectra (19).

SUPPORTING INFORMATION

The following files are available free of charge: simulated TD-DFT spectra, LUMO diagrams, maximum and minimum rotational energy plots and geometries, Mulliken Population Analysis and Kohn-Sham Orbital tables.

AUTHOR INFORMATION

Corresponding Author

*Pierre Kennepohl (pierre.kennepohl@ucalgary.ca)

Author Contributions

The manuscript was written through contributions of all authors. All authors have given approval to the final version of the manuscript.

ACKNOWLEDGMENT

We thank Scott Bohle for providing us the compound tert-butanesulfonamide; Matthew Latimer and Erik Nelson at SSRL Beamline 4-3; and Yongfeng Hu at CLS Beamline SXRMB. Use of the Stanford Synchrotron Radiation Lightsource, SLAC

National Accelerator Laboratory, is supported by the U.S. Department of Energy, Office of Science, Office of Basic Energy Sciences under Contract No. DE-AC02-76SF00515. The SSRL Structural Molecular Biology Program is supported by the DOE Office of Biological and Environmental Research, and by the National Institutes of Health, National Institute of General Medical Sciences (P41GM103393). The contents of this publication are solely the responsibility of the authors and do not necessarily represent the official views of NIGMS or NIH and Part of the research described in this paper was performed at the Canadian Light Source, a national research facility of the University of Saskatchewan, which is supported by the Canada Foundation for Innovation (CFI), the Natural Sciences and Engineering Research Council (NSERC), the National Research Council (NRC), the Canadian Institutes of Health Research (CIHR), the Government of Saskatchewan, and the University of Saskatchewan.

ABBREVIATIONS

XAS, X-ray Absorption Spectroscopy; TD-DFT, Time Dependent - Density Functional Theory

Bibliography

1. N-tert-butanesulfinyl imines: versatile intermediates for the asymmetric synthesis of amines. Ellman, Jonathan A. and Owens, Timothy D. and Tang, Tony P. 11, 2002, *Accounts of Chemical Research*, Vol. 35, pp. 984--995.
2. The Safety Catch Principle in Solid Phase Peptide Synthesis. Kenner, G.W. and McDermott, J.R. and Sheppard, R.C. 1971, *Chemical Communications*, Vol. 12, pp. 636--637.
3. Carbonic Anhydrase Inhibitors. Supuran, Claudiu T., Scozzafava, Andrea and Casini, Angela. 2, 2003, *Medicinal Research Reviews*, Vol. 23, pp. 146--189.
4. A NMR study of the binding of novel N-hydroxybenzenesulfonamide carbonic anhydrase inhibitors to native and cadmium-111-substituted carbonic anhydrase. Blackburn, G. Michael, et al. 1985, *European Journal of Biochemistry*, Vol. 153, pp. 553--558.
5. Physicochemical and structural properties of bacteriostatic sulfonamides: theoretical study. Soriano-Correa, Catalina, Esquivel, Rodolfo O. and Sagar, Robin P. 2003, *International Journal of Quantum Chemistry*, Vol. 94, pp. 165--172.
6. Dihydroquinolones—V: Hindered inversion in dihydroquinolones and related systems. Speckamp, W.N. and Pandit, U.K. and Korver, P.K. and van der Haak, P.J. and Huisman, H.O. 8, 1966, *Tetrahedron*, Vol. 22, pp. 2413--2427.
7. Chemical Bonding in Hypervalent Molecules. The Dominance of Ionic Bonding and Negative Hyperconjugation over d-orbital Participation. Reed, Alan E. and von Rague Schleyer, Paul. 4, 1990, *Journal of the American Chemical Society*, Vol. 112, pp. 1433--1445.
8. The Effect of Polar Substituents on the Barrier to Rotation about the Sulfonyl Sulfur-Nitrogen Bond in {N}-Alkyl-{N}-arenesulfonylarenesulfenamides. Raban, Morton and Jones Jr., Freeman B. 11, 1971, *Journal of the American Chemical Society*, Vol. 93, pp. 2692--2699.

9. Study of Unusually High Rotational Barriers About S-N Bonds in Nonafluorobutane-1-sulfonamides: The Electronic Nature of the Torsional Effect. Lyapkalo, Ilya M. and Reissig, Hans-Ulrich and Schafer, Andreas and Wagner, Armin. 2002, *Helvetica Chimica Acta*, Vol. 85, pp. 4206--4215.
10. Conformational Analysis of Substituted Hexahydropyrrolo [2,3-b]indoles and Related Systems. An Unusual Example of Hindered Rotation about Sulfonamide S-N Bonds. An X-ray Crystallographic and NMR Study. Crich, David, et al. 8, 1995, *Tetrahedron*, Vol. 51, pp. 2215--2228.
11. Natural Abundance Nitrogen-15 NMR spectroscopy. Electronic Effects in Benzenesulfonamides. Schuster, Ingeborg I. and Doss, Senot H. and Roberts, John D. 25, 1978, *Journal of Organic Chemistry*, Vol. 43, pp. 4693--4696.
12. Electronic structure of S-nitrosothiols from sulfur K-edge x-ray absorption spectroscopy. Martin-Diaconescu, Vlad and Perepichka, Inna and Bohle, Scott and Kennepohl, Pierre. 2011, *Canadian Journal of Chemistry*, Vol. 89, pp. 93--97.
13. Sulfur K-edge x-ray absorption spectroscopy as an experimental probe for S-nitroso proteins. Szilagyi, Robert K. and Schwab, David E. 2005, *Biochemical and Biophysical Research Communications*, Vol. 330, pp. 60--64.
14. Resonance Description of S-Nitrosothiols: Insights into Reactivity. Timerghazin, Qadir K., Peshherbe, Gilles H. and English, Ann M. 16, 2007, *Organic Letters*, Vol. 9, pp. 3049--3052.
15. Redox photochemistry of methionine by sulfur K-edge x-ray absorption spectroscopy: potential implications for cataract formation. Karunakaran-Datt, Anusha and Kennepohl, Pierre. 2009, *Journal of the American Chemical Society*, Vol. 131, pp. 3577--3582.
16. Ligand K-edge x-ray absorption spectroscopy as a probe of ligand-metal bonding: charge donation and covalency in copper-chloride systems. Shadle, Susan E. and Hedman, Britt and Hodgson, Keith O. and Solomon, Edward I. 1994, *Inorganic Chemistry*, Vol. 33, pp. 4235--4244.
17. Effects of Hyperconjugation on the Electronic Structure and Photoreactivity of Organic Sulfonyl Chlorides. Martin-Diaconescu, Vlad and Kennepohl, Pierre. 2009, *Inorganic Chemistry*, Vol. 48, pp. 1038--1044.
18. This feature is due to photoreduction during exposure.
19. Calibration of Scalar Relativistic Density Functional Theory for the Calculation of Sulfur {K}-Edge Absorption Spectra. George, Serena DeBeer and Neese, Frank. 2010, *Inorganic Chemistry*, Vol. 49, pp. 1849--1853.
20. Theoretical studies on S-N interactions in sulfonamides. Bharatam, Prasad V. and Gupta, Amita and Gupta, Arti and Kaur, Damanjit. 2002, *Tetrahedron*, Vol. 58, pp. 1759--1764.
21. Ligand K-edge x-ray absorption spectroscopy: covalency of ligand-metal bonds. Solomon, Edward I., et al. 2005, *Coordination Chemistry Reviews*, Vol. 249, pp. 97--129.
22. Blueprint XAS: a Matlab-based toolbox for the fitting and analysis of XAS spectra. Delgado-Jaime, Mario Ulises and Mewis, Craig Philip and Kennepohl, Pierre. 2010, *Journal of Synchrotron Radiation*, Vol. 17, pp. 132--137.
23. Development and exploration of a new methodology for the fitting and analysis of {XAS} data. Delgado-Jaime, Mario Ulises and Kennepohl, Pierre. 2010, *Journal of Synchrotron Radiation*, Vol. 17, pp. 119--128.
24. A new look at the statistical model identification. Akaike, Hirotugu. 6, 1974, *IEEE Transactions on Automatic Control*, Vol. 19, pp. 716--723.
25. An information-based computational technique for estimation of chromatographic peak purity. Lun, Desmond S and Jennings, Laura D and Koetter, Ralf and Licht, Stuart and Médard, Muriel. 5, 2007, *Journal of Chemical Information and Modeling*, Vol. 47, pp. 1973--1978.
26. The ORCA program system. Neese, Frank. 2011, *Wiley Interdisciplinary Reviews: Computational Molecular Science*, Vol. 2, pp. 73--78.